

Energy-transfer rate in a double-quantum-well system due to Coulomb coupling

R. T. Senger and B. Tanatar

Department of Physics, Bilkent University, Bilkent, 06533 Ankara, Turkey

We study the energy-transfer rate for electrons in a double-quantum-well structure, where the layers are coupled through screened Coulomb interactions. The energy-transfer rate between the layers (similar to the Coulomb drag effect in which the momentum transfer rate is considered) is calculated as functions of electron densities, interlayer spacing, the temperature difference of the 2DEGs, and the electron drift velocity in the drive layer. We employ the full wave vector and frequency dependent random-phase approximation at finite temperature to describe the effective interlayer Coulomb interaction. We find that the collective modes (plasmons) of the system play a dominant role in the energy transfer rates. The contribution of optical phonons to the transfer rates through the phonon mediated Coulomb coupling mechanism has also been considered.

PACS numbers: 72.10.-d, 73.50.Dn, 73.25.Dx, 73.20.Mf

I. INTRODUCTION

Coupled quantum-well systems are known to exhibit rich and interesting physics, where correlation effects are significant.¹ In particular, the Coulomb drag effect is a unique way of probing many-body correlations through a transport measurement,²⁻⁴ where one of the layers is driven by an external current, and the influences on the other (drag) layer are investigated. The inter-layer carrier-carrier interactions lead to measurable effects, such as transresistivity due to momentum transfer between the layers. The observed transresistance crucially depends on the single-particle and collective excitations of the coupled system, because these excitations are the ones which mediate the momentum and energy transfer between the layers. There has been a growing theoretical⁵⁻⁸ and experimental⁹⁻¹² activity in the past years touching upon various aspects of the drag phenomenon.

In this paper we study the energy transfer between two layers of quasi-two-dimensional electron gases under experimental conditions similar to the transresistivity measurements. The importance of the energy transfer between two Coulomb coupled quantum wells were pointed out by Price.^{13,14} In the hot-electron context, the energy transfer occurs when there is a difference of electron temperatures in the two layers. In the actual drag experiments^{9,15} the energy transfer was detected from the heating effects. The energy transfer rate in spatially separated systems were theoretically considered also by Jacobini and Price,¹⁶ Laikhtman and Solomon,¹⁷ Boiko and Sirenko,¹⁸ and recently by Tanatar¹⁹ who considered the case of a coupled quantum wire system.

We calculate the temperature dependence of the energy transfer rate in a double quantum well system. It is assumed that the wells may be kept at different carrier temperatures which are also different from the lattice

temperature in general.²⁰ The calculations are based on the random-phase approximation (RPA), with full consideration of wave vector and frequency dependencies at finite temperatures. The layers are coupled through Coulomb interactions, and in the steady state the resulting charge polarization produces an electrostatic field which compensates the drag force in the drag layer. Using the momentum and energy balance equations we investigate the static and dynamic screening effects on the power transfer between the layers. In the drive layer the influence of the externally applied electric field is treated in terms of the electron drift velocity. We probe the effects of a finite drift velocity to study the nonlinear regime of the energy transfer rate. The nonequilibrium aspects of frictional drag has recently been considered by Wang and da Cunha Lima,²¹ who employed the balance equation approach. The amount of transferred energy has a direct dependence on the electron layer densities which can be different in general. We also calculate the effect of density mismatch on the energy transfer rates. As a final point to be discussed in this report we consider the contribution of optical phonon exchange as an additional mechanism of interlayer interaction.

II. MODEL

We consider two quantum wells of width w , and center-to-center separation of d . The potential barriers are assumed to be infinite, so that there is no tunneling between the layers. The two dimensional electron charge density in the first layer, n_1 , is related to the Fermi wave vector by $n_1 = k_F^2/(2\pi)$, and T_F is the corresponding Fermi temperature of the electron gas in the layer. It is also appropriate to define the dimensionless electron gas parameter $r_s = \sqrt{2}/(k_F a_B^*)$, where $a_B^* = \epsilon_0/(e^2 m^*)$ is the effective Bohr radius in the layer material with background

dielectric constant ϵ_0 and electron effective mass m^* . For GaAs quantum-wells $a_B^* \approx 100 \text{ \AA}$ and experimentally realized electron densities are of the order of 10^{11} cm^{-2} which corresponds to $r_s \approx 1-2$, and $T_F \approx 40-100 \text{ K}$. We take the charge density in the second layer with reference to the drive layer; $n_2 = \alpha n_1$, so that the quantities for the second layer scale as, $k_F^{(2)} = \sqrt{\alpha} k_F$, $r_s^{(2)} = r_s / \sqrt{\alpha}$, $T_F^{(2)} = \alpha T_F$.

The transport properties of the double quantum well system can be characterized by the electron drift velocities v_i and electron gas temperatures T_i . One of the layers (drive layer) is subject to an electric field in the x -direction which drives the electrons with a drift velocity v_1 . The other well is kept as an ‘‘open circuit’’, therefore $v_2 = 0$. The drag experiments are performed at low electric fields in the linear regime, so we shall take the limit $v_1 \rightarrow 0$ at the end of the calculations. In this work our starting point for the calculation of the energy transfer rate is the balance-equation approach to hot carrier transport which has been successfully applied to a variety of situations involving transport phenomena in semiconductors.²² The resulting momentum and energy transfer rate equations have also been obtained within a variety of other techniques.^{3,5,6,18} With the assumption that only the lowest subband in each layer is occupied, the momentum and energy transfer rate expressions due to interlayer Coulomb interactions, derived within the balance equation approach to nonlinear electrical transport in low dimensional semiconductors, are given by²⁰⁻²² ($\hbar = k_B = 1$);

$$f_{12}(v_1 - v_2) = - \sum_{\vec{q}} q_x \int_{-\infty}^{\infty} \frac{d\omega}{\pi} |W_{12}(q, \omega)|^2 \times \left[n_B \left(\frac{\omega}{T_1} \right) - n_B \left(\frac{\omega - \omega_{12}}{T_2} \right) \right] \times \text{Im}\chi_1(q, \omega) \text{Im}\chi_2(-q, \omega_{12} - \omega), \quad (1)$$

and

$$P_{12}(v_1 - v_2) = - \sum_{\vec{q}} \int_{-\infty}^{\infty} \frac{d\omega}{\pi} \omega |W_{12}(q, \omega)|^2 \times \left[n_B \left(\frac{\omega}{T_1} \right) - n_B \left(\frac{\omega - \omega_{12}}{T_2} \right) \right] \times \text{Im}\chi_1(q, \omega) \text{Im}\chi_2(-q, \omega_{12} - \omega) \quad (2)$$

respectively. In the above, $\omega_{12} = q_x(v_1 - v_2)$, $W_{12}(q, \omega) = V_{12}(q)/\epsilon(q, \omega)$ is the dynamically screened interlayer potential, $\text{Im}\chi(q, \omega)$ is the imaginary part of the temperature dependent 2D susceptibility³ for a single layer, and $n_B(x) = 1/(\exp(x) - 1)$ is the Bose distribution function. The screening function $\epsilon(q, \omega)$ for the double-well system is written as

$$\epsilon(q, \omega) = [1 - V_{11}(q)\chi_1(q, \omega; T_1)][1 - V_{22}(q)\chi_2(q, \omega; T_2)] - V_{12}^2(q)\chi_1(q, \omega; T_1)\chi_2(q, \omega; T_2), \quad (3)$$

where

$$V_{ij}(q) = F_{ij}(qw) \frac{2\pi e^2}{\epsilon_0 q} e^{-qd(1-\delta_{ij})} \quad (4)$$

define the intra- and interlayer unscreened Coulomb interactions, and $F_{ij}(qw)$ are the form factors^{3,6} for a model of infinite barrier and square wells of width w . Note that we have indicated explicitly in Eqs.(1) and (2) that the layers or quantum-wells are kept at different temperatures. Under drag conditions mentioned above, the interlayer resistivity (transresistivity) reads

$$\rho_{12} = - \frac{1}{n_1 n_2 e^2 v_1} f_{12}(v_1), \quad (5)$$

where f_{12} is the interlayer momentum transfer rate or frictional force. Resistivity expression is further simplified if we consider layer temperatures to be equal, $T_1 = T_2$, and within the linear regime $v_1 \rightarrow 0$, yielding

$$\rho_{12} = - \frac{1}{n_1 n_2 e^2} \left. \frac{df_{12}(v_1)}{dv_1} \right|_{v_1=0}. \quad (6)$$

The energy transfer rate expression given in Eq.(2) resembles the momentum transfer rate expression of Eq.(1), except the transferred energy ω appears in the integrand, and the difference between the Bose distribution functions at different temperatures reduce to the familiar^{2,5,6} $\sim 1/\sinh^2(\omega/2T)$ when T_1 approaches T_2 . With the sign chosen in Eq.(2), P_{12} is the amount of power transferred to the layer 1 from the layer 2.

III. RESULTS AND DISCUSSION

We first evaluate the energy-transfer rate $P_{12}(0)$ in the linear regime ($v_1 = 0$) for a GaAs system. Even in this case, the energy transfer rate is non-zero as long as the electron gases are kept at different temperatures. The comparison of taking the interlayer potential as either statically or dynamically screened is presented in Fig.1(a). Because the energy transfer rate P_{12} changes sign as T_2 is scanned for a fixed T_1 , we plot $|P_{12}|$ in our presentations. In the statically screened interaction we use $\epsilon(q) = [1 - V_{11}\chi_1(q)][1 - V_{22}\chi_2(q)] - V_{12}^2\chi_1(q)\chi_2(q)$, in which the static response functions $\chi_{1,2}(q, \omega = 0)$ enter. Both quantum wells are taken of width $w = 2a_B^*$, and with equal electron densities ($n_1 = n_2$). The temperature of the first layer is kept at $T_1 = T_F$. For three distinct sets of r_s and d values, the T_2 dependence of $|P_{12}|$ is plotted. We observe that the inclusion of dynamical screening effects yields qualitatively and quantitatively different results for the energy transfer rate. At very low T_2 both types of screening yield close results, but with the increasing temperature, P_{12} significantly grows for dynamical screening, whereas it monotonically decreases for the case of static screening. The difference between the two approaches is attributed to the contribution of plasmons

which is completely missed for the statically screened interaction. Similar differences between the static and dynamic screening approaches were also found in the momentum transfer rate at high temperatures determining the transresistivity.³ We notice that the qualitative forms of the curves are roughly independent of the separation distance and the charge density. When the temperatures of both layers are equal the energy transfer vanishes for all cases in the linear regime. This is also seen in Fig. 1(b) where we take T_1 at three different values, and vary T_2 from 0 to T_F . Although experimentally the energy transfer is expected to be from the drift layer to the drag layer (in the linear regime at least), for the sake of generality the cases where $T_2 > T_1$ are also included in our plots. Note that P_{12} changes sign when $T_2 > T_1$, so that energy is transferred from the hot layer to the cold one. When we compare the overall behavior of P_{12} in a double-layer system with that in a coupled quantum wire system, we observe that in the latter a pronounced peak structure¹⁹ around $T \sim 0.3 T_F$ is present. On the other hand, the results shown in Figs. 1(a) and 1(b) indicate a rather broad enhancement coming from the plasmon excitations. Price has estimated¹⁴ the energy transfer rate (per electron) between coupled quantum wells to be $\sim 0.1 - 1$ erg/s, for typical layer densities of $n \sim 10^{11} \text{ cm}^{-2}$ and $d \approx 100 \text{ \AA}$. In obtaining this estimate, the electron temperature was taken as 10^3 K , which is about $10 T_F$. Our calculations are mostly done for layers of finite thickness, larger separation distances and at relatively lower temperatures around T_F . The results indicate rates of the order of 10^{-2} erg/s, which are much smaller than the estimate given by Price.¹⁴

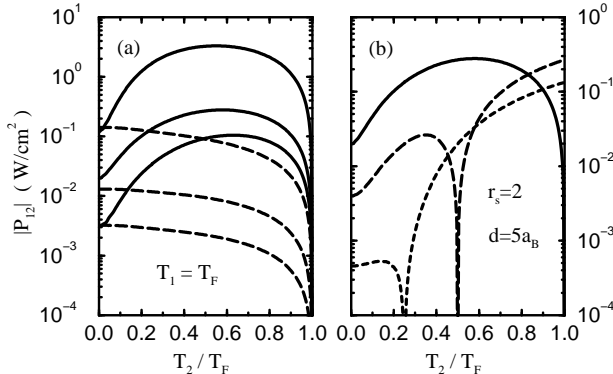


FIG. 1. The energy-transfer rate for identical quantum-wells of width $w = 2a_B^*$, (a) in the static (dashed) and the dynamic (solid) screening approximations as functions of temperature T_2 . The temperature of the drive layer is kept constant at $T_1 = T_F$. The couple of curves from top to bottom are for (r_s, d) values of $(1, 5a_B^*)$, $(2, 5a_B^*)$ and $(2, 7a_B^*)$ respectively, (b) for different values of T_1 . The solid, dashed, and short-dashed curves are for $T_1/T_F = 1, 0.5$, and 0.25 , respectively.

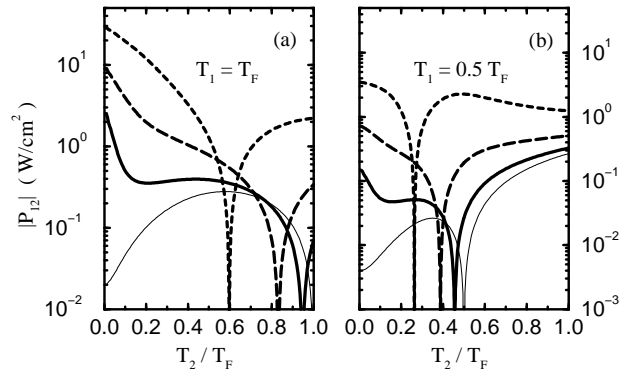


FIG. 2. The energy-transfer rate for identical wells in the nonlinear regime when (a) $T_1 = T_F$, (b) $T_1 = 0.5 T_F$. The solid, dashed, and short-dashed curves are for $v_1 k_F / E_F = 0.5, 1$, and 2 , respectively, in a $w = 2a_B^*$ and $d = 5a_B^*$ double-well system ($r_s = 2$). The thin solid curves correspond to the linear regime ($v_1 = 0$), included for comparison.

Next we investigate the energy-transfer rate in the nonlinear regime (i.e. for non-zero v_1). The density response function and the Bose distribution function of the drag layer are calculated at shifted frequencies $\omega - q_x v_1$. In Fig. 2 the energy transfer rate is displayed in this nonlinear situation when T_1 is kept at either T_F or $0.5 T_F$. We observe that for a finite drift velocity and at very low temperatures of the second layer, the amount of transferred power is a few orders of magnitude larger than that for the linear regime. As T_2 is increased, $|P_{12}|$ starts to decrease rapidly and eventually vanish at a critical value, before the temperatures of the layers become equal. Larger the drift velocity lower the T_2 at which no energy is transferred between the layers (eg. for $T_1 = T_F$ and $v_1 = 2E_F/k_F$, $P_{12} = 0$ at $T_2 \approx 0.6 T_F$). Beyond that point, as a consequence of nonlinearity, for further larger values of T_2 the drive layer start to *absorb* power from the second layer even when $T_1 > T_2$. The momentum transfer rate between two coupled electron-hole quantum wells in the nonlinear regime was considered by Cui, Lei, and Horing.²⁰ They found that the nonlinear effects start to become significant at different electric field strengths (or equivalently the drift velocity v_1) for different temperatures. In a system of two sets of charged particles streaming relative to one another the collective modes may undergo instabilities with respect to charge density perturbations as studied by Hu and Wilkins.²³ It is conceivable that under the drag effect conditions, such two-stream instabilities may be detected for large drift velocities. Hu and Flensberg²⁴ predicted a significant rise in the drag rate just under the instability threshold. Recent drag rate calculations of Wang and da Cunha Lima²¹ did not explore this phenomenon. In our calculations of the energy transfer rate, the shift of vanishing P_{12} point to lower T_2 values is expected to reflect the onset of plasma instabilities. In our numerical results shown in Figs. 2(a) and 2(b) it appears that two-stream instability limit is

not yet reached for the drift velocities chosen.

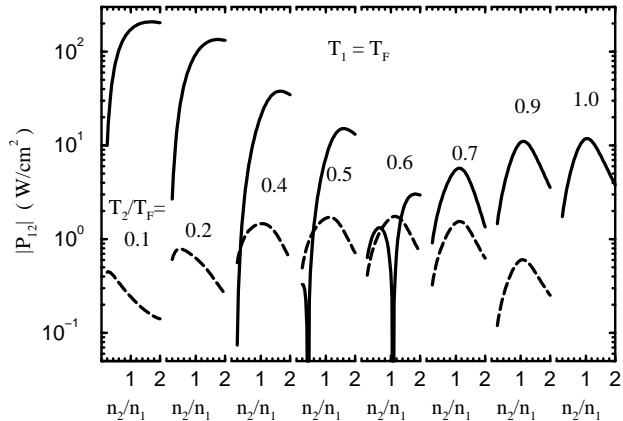


FIG. 3. The energy-transfer rate as functions of the ratio of drag/drive layer electron densities n_2/n_1 at different drag-layer temperatures T_2 , and for electron density $n_1 = 2 \times 10^{11} \text{ cm}^{-2}$ ($r_s = 1.22$). The dashed and solid curves are for the linear and nonlinear ($v_1 = 2E_F/k_F$) regimes, respectively. We take $w = 2a_B^*$ and $d = 5a_B^*$. Note that in the linear regime $P_{12} = 0$ when $T_1 = T_2$, regardless of the density ratio.

The effect of charge density mismatch in the two layers on the energy-transfer rate is shown in Fig. 3. We keep $n_1 = 2 \times 10^{11} \text{ cm}^{-2}$ ($r_s = 1.22$) and $T_1 = T_F$ constant, and vary n_2/n_1 in the range 0.2 to 2 for different T_2 values. Both in the linear and nonlinear regimes it is observed that P_{12} is very sensitive to the electron density ratio of the layers. For relatively large temperatures ($T_2 \sim T_F$) the energy-transfer is considerably larger when the densities are equal. In the linear regime (cf, dashed curves in Fig. 3), the peak value of P_{12} shifts to smaller values of n_2/n_1 ratio when the temperature of the second layer is lowered, for example at $T_2 = 0.1T_F$ the largest transfer rates occur for $n_2 \approx 0.2n_1$. For finite drift velocities the nonlinear effects show up also in terms of the density ratio. The vanishing of power transfer at finite temperature differences of the layers is seen at even lower T_2 if $n_2 < n_1$. In the figure, for $v_1 k_F/E_F = 2$, the direction of energy flow is from layer 1 to layer 2 ($P_{12} < 0$) if $T_2 \leq 0.4T_F$, and vice versa if $T_2 \geq 0.7T_F$ in the chosen range of the density ratio. For the cases $T_2 = 0.5T_F$ or $0.6T_F$ however, $P_{12} < 0$ at larger values of n_2 , and changes sign at certain values of the density ratio, as n_2 is lowered. The feature is due to that a constant temperature corresponds to a larger effective temperature for a lower-density electron gas, in units of the Fermi temperature of the second layer. The momentum transfer rate in the drag phenomenon has been known to be very sensitive to the relative densities in the spatially separated electron systems.^{4,12,21} We find here that energy transfer rate also has a strong dependence on the ratio n_2/n_1 .

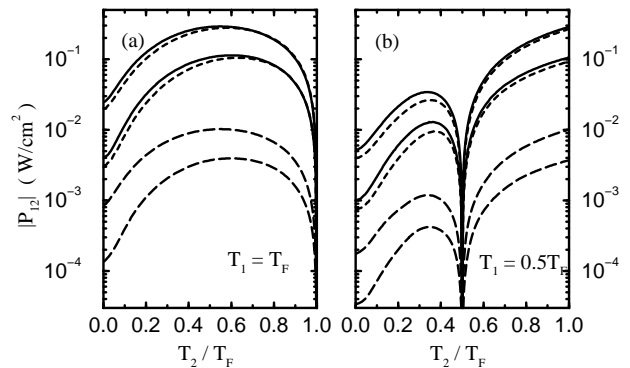


FIG. 4. Comparison of Coulomb and optical phonon mediated Coulomb interaction mechanisms in the energy transfer rate. The short- and long-dashed curves are, respectively, for Coulomb-only and phonon-only contributions to the energy transfer rates. The solid curves represent the simultaneous inclusion of both mechanisms. The upper and lower curves of each type are for $d = 5a_B^*$ and $d = 7a_B^*$ respectively. ($n_1 = n_2$, $r_s = 2$ and $w = 2a_B^*$)

Finally, we calculate the effect of optical phonons on the energy transfer rate in a double-layer electron system. At low temperatures, the acoustic phonons are known to contribute to the momentum transfer rate.²⁵ Since we are more interested in the high temperature regime where plasmons play a dominant role in the momentum and energy transfer rates, we consider only the dispersionless optical phonons for the phonon mediated interlayer electron-electron interactions. More specifically, we replace the interlayer effective electron-electron interaction by

$$W_{12}(q, \omega) = \frac{V_{12}(q) + D_{12}(q, \omega)}{\epsilon_T(q, \omega)} \quad (7)$$

to account for the Coulomb and LO-phonon mediated interactions simultaneously. The phonon term D_{12} which also has a Coulombic nature is calculated to be^{26,27}

$$D_{12}(q, \omega) = V_{12}(q) \left(1 - \frac{\epsilon_\infty}{\epsilon_0} \right) \frac{\omega_{\text{LO}}^2}{\omega^2 - \omega_{\text{LO}}^2 + i\gamma\omega}. \quad (8)$$

The above form of the interaction due to the exchange of virtual phonons arise when the “bubble” diagrams to all orders are considered within the RPA. Here γ^{-1} is the phenomenological lifetime for phonons. γ is taken finite in our calculations but the results do not have a significant dependence on γ as long as it is small (i.e. for GaAs, $\gamma \sim 0.1 \text{ meV}$, whereas $\omega_{\text{LO}} = 36 \text{ meV}$). The total screening function is modified in a straightforward way to include the phonon contribution,

$$\epsilon_T(q, \omega) = [1 - (V_{11} + D_{11})\chi_1] [1 - (V_{22} + D_{22})\chi_2] - (V_{12} + D_{12})^2 \chi_1 \chi_2. \quad (9)$$

D_{ii} are the phonon mediated intralayer electron-electron interaction terms defined similar to D_{12} . The zeros of

the total screening function $\varepsilon_T(q, \omega)$ give the coupled plasmon-phonon mode dispersions. The purely Coulomb and phonon mediated interaction contributions to the amount of transferred energy are not simply additive, due to the interference terms coming from the total interaction amplitude, Eq. (7). It is possible to consider the phonon contribution alone by keeping only the D_{12} term in the numerator of Eq. (7), i.e. $W_{12}(q, \omega) = D_{12}/\varepsilon_T$. However one should retain²⁸ the coupling of Coulomb and phonon terms in $\varepsilon_T(q, \omega)$.

We calculate the energy transfer rate between two quantum wells by modifying the expression for P_{12} as set out above for the phonon mediated Coulomb interaction. We assume that electrons and phonons are in thermal equilibrium at T_1 . In Fig. 4 we display the energy-transfer rates due to the Coulomb and phonon coupling interactions alone, and when both mechanisms are present together. It is observed that the phonon contribution, being almost an order of magnitude smaller, has qualitatively similar form as the direct Coulomb interaction contribution. The mentioned interference is observable when the temperature difference of the layers is small; the combined effect of two mechanisms can lead to slightly smaller transfer rates (cf, Fig. 4(a)).

In summary, we have considered the energy transfer rate in a double-quantum-well system in a drag experiment type setup. The interlayer Coulomb scattering mechanism through dynamical screening effects greatly enhances the energy transfer rate from one layer to another. We have found that a large drift velocity corresponding to large externally applied field greatly modifies the energy transfer rate and may lead to power absorption from the cooler electron gas to the other. Some of our predictions may be tested in hot-electron photoluminescence experiments, in which the power loss of an electron gas is measured. Lastly, we have also considered the contribution of optical phonons in the phonon mediated Coulomb drag which may be important to understand the future experiments. It would be interesting to extend the measurements of Noh *et al.*²⁵ to higher temperatures to observe the effects of coupled plasmon-phonon modes.

ACKNOWLEDGMENTS

This work was partially supported by the Scientific and Technical Research Council of Turkey (TÜBİTAK) under Grant No. TBAG-2005, by NATO under Grant No. SfP971970., and by the Turkish Department of Defense under Grant No. KOBRA-001. We thank Dr. P. J. Price for his useful comments.

- ¹ See for recent reviews, L. Świerkowski, D. Neilson, and J. Szymański, *Aust. J. Phys.* **46**, 423 (1993); C. B. Hanna, D. Haas, and J. C. Díaz-Vélez, *Phys. Rev. B* **61**, 13 882 (2000).
- ² A. G. Rojo, *J. Phys.: Condens. Matter* **11**, R31 (1999).
- ³ K. Flensberg and B. Y.-K. Hu, *Phys. Rev. B*, **52**, 14796 (1995).
- ⁴ N.P.R. Hill, J.T. Nichols, E.H. Linfeld, K.M. Brown, M. Pepper, D.A. Ritchie, G.A.C. Jones, B.Y. Hu, K. Flensberg, *Phys. Rev. Lett.* **78**, 2204 (1997).
- ⁵ L. Zheng and A. H. MacDonald, *Phys. Rev. B* **48**, 8203 (1993).
- ⁶ A.-P. Jauho and H. Smith, *Phys. Rev. B* **47**, 4420 (1993).
- ⁷ H. C. Tso, P. Vasilopoulos, and F. M. Peeters, *Phys. Rev. Lett.* **68**, 2516 (1992).
- ⁸ A. Kamenev and Y. Oreg, *Phys. Rev. B* **52**, 7516 (1994).
- ⁹ P. M. Solomon, P. J. Price, D. J. Frank, and D. C. La Tulipe, *Phys. Rev. Lett.* **63**, 2508 (1989).
- ¹⁰ T. J. Gramila, J. P. Eisenstein, A. H. MacDonald, L. N. Pfeiffer, and K. W. West, *Phys. Rev. Lett.* **66**, 1216 (1991).
- ¹¹ U. Sivan, P. M. Solomon, and H. Shtrikman, *Phys. Rev. Lett.* **68**, 1196 (1992).
- ¹² H. Noh, S. Zelakiewicz, X. G. Feng, T. J. Gramila, L. N. Pfeiffer, and K. W. West, *Phys. Rev. B* **58**, 12 621 (1998).
- ¹³ P. J. Price, *Physica B* **117**, 750 (1983).
- ¹⁴ P. J. Price, in *Physics of Submicron Semiconductor Devices*, edited by H. L. Grubin, D. K. Ferry, and C. Jacobini (Plenum, New York, 1988).
- ¹⁵ P. M. Solomon and B. Laikhtman, *Superlattices Microstruct.* **10**, 89 (1991).
- ¹⁶ C. Jacobini and P. J. Price, *Solid State Electronics* **31**, 649 (1988).
- ¹⁷ B. Laikhtman and P. M. Solomon, *Phys. Rev. B* **41**, 9921 (1990).
- ¹⁸ I. I. Boiko and Yu. M. Sirenko, *Phys. Status Solidi B* **159**, 805 (1990).
- ¹⁹ B. Tanatar, *J. Appl. Phys.* **81**, 6214 (1997).
- ²⁰ H. L. Cui, X. L. Lei, and N. J. M. Horing, *Superlattices Microstruct.* **13**, 221 (1993)
- ²¹ X. F. Wang and I. C. da Cunha Lima, preprint cond-mat/0011394.
- ²² *Physics of Hot Electron Transport in Semiconductors*, edited by C. S. Ting (World Scientific, Singapore, 1992)
- ²³ B. Y.-K. Hu and J. W. Wilkins, *Phys. Rev. B* **43**, 14 009 (1991).
- ²⁴ B. Y.-K. Hu and K. Flensberg, in *Hot Carriers in Semiconductors*, edited by K. Hess, J.-P. Leburton, and U. Ravaioli (Plenum, New York, 1996).
- ²⁵ H. Noh, S. Zelakiewicz, T. J. Gramila, L. N. Pfeiffer, and K. W. West, *Phys. Rev. B* **59**, 13 114 (1999).
- ²⁶ K. Güven and B. Tanatar, *Phys. Rev. B* **56**, 7535 (1997).
- ²⁷ B. Y.-K. Hu, *Phys. Rev. B* **57**, 12 345 (1998).
- ²⁸ M. C. Bønsager, K. Flensberg, B. Y.-K. Hu and A. H. MacDonald, *Phys. Rev. B* **57**, 7085 (1998).